Optica Applicata, Vol. XXXII, No. 4, 2002

Automatic polarimetric system for early medical diagnosis by biotissue testing

ROMUALD JÓŹWICKI, KRZYSZTOF PATORSKI

Institute of Micromechanics and Photonics, Faculty of Mechatronics, Warsaw University of Technology, ul. Chodkiewicza 8, 02–525 Warszawa, Poland.

OLEG V. ANGELSKY, ALEXANDER G. USHENKO, DIMITRY N. BURKOVETS, YURIY A. USHENKO

Correlation Optics Department, Chernivtsi National University, 2 Kotsyubinsky Str., 58012 Chernivtsi, Ukraine.

An automatic polarimetric system constructed at the Optical Engineering Division of the Warsaw University of Technology (Poland) and the evaluation method developed at the Department of Correlation Optics of Chernivtsi State University (Ukraine) are presented. The polarimeter has been designed and constructed to test the biotissues in the form of biopsy samples. After the system autocalibration the isocline and isochrome images are registered automatically. Correlation characteristics of the images calculated by the computer program provide the basis for formulating the medical diagnosis.

1. Automatic polarimeter design

The task of the polarimeter is to test the structural elements of anisotropic tissues acquired by the conventional biopsy method. The overall layout of the instrument is shown in Fig. 1 and its photograph in Fig. 2. The main optical elements of the polarimeter are the He-Ne laser ($\lambda = 0.6328$ μm, 10 mW), the polaroid P, two quartz -made quarter-wave ($\lambda/4$) plates (4th order) and the polaroid A as the analyser. By setting the polarisation plane of P parallel to the optical axis of the first quarter-wave plate the object under test O (a tissue sample) is illuminated by a linearly polarised light beam. With the analyser similarly coupled with the second quarter-wave plate the isoclines can be analysed. For that purpose the analyser has its transmittance plane perpendicular to the analyser one (in that case, with no anisotropic object present, the light behind the analyser is completely extinguished). The isoclines form a set of lines (fringes) over the object area representing the geometric locus of the local optical axis orientations parallel to the plane of polarisation of the incident beam.

By setting the optical axes of both quarter-wave plates at 45° with respect to linear polarisation plane of the light beam, the circular polarisation in front of the object under test is obtained. Now, the isochromatic lines (a family of lines corresponding to constant phase differences introduced by anisotropic elements found in the biotissue) can be studied.

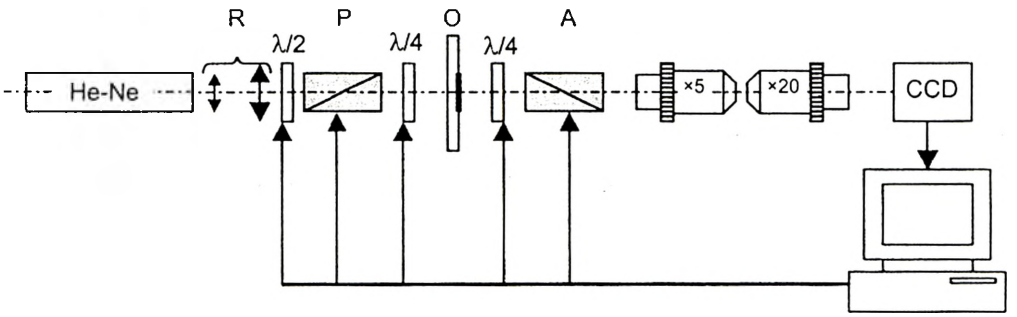

Fig. 1. Overall layout of the polarimeter.

The He-Ne laser beam is expanded by the afocal system R up to the diameter of 3 mm. The pinhole located in the expansion optics removes the scattered light originating from secondary reflections in the resonator and optics contaminations. The role of the half-wave plate $\lambda/2$ is to match the laser beam polarisation plane to the polariser transmittance direction and, at the same time, to control the light intensity level at the CCD matrix to avoid its saturation.

The tissue sample is placed on the microscope slide and covered with the microscope cover glass. The slide with tissue is fixed in a mount providing transverse translations in two mutually perpendicular directions in the range of 5 mm to enable the choice of various fragments of the sample.

The sample image is formed on the CCD matrix by the optical system composed of two microscope objectives. The lateral magnification of the imaging system dictated by the matrix and lateral dimensions of an object under test is equal to 4. The overall dimensions of the quarter-wave and analyser driving systems do not allow the imaging optics to be placed closer than 200 mm away from the sample. Introducing any optical element in front of the analyser is not recommended since even its residual level birefringence would cause the measurement error. The set of two microscope objectives permits obtaining lateral magnification factor mentioned above without the necessity of an excessive axial elongation of the imaging optics. The images registered by the CCD matrix and the frame grabber are transferred in a digital form to the computer memory.

The half-wave plate, both quarter-wave plates, the polariser and analyser are rotated by means of step motors. One motor step corresponds to 22.5 minutes of arc of the rotation of an optical element. The motors are controlled by a D/A card housed in the computer. Two operation modes are possible: automatic mode according to the software developed and manual mode using the keyboard.

Before making measurements the automatic system calibration is performed in the following order:

– the optical axes of quarter-wave plates are set parallel to transmittance directions of polariser and analyser,

– the transmittance planes of polariser and analyser are set parallel,

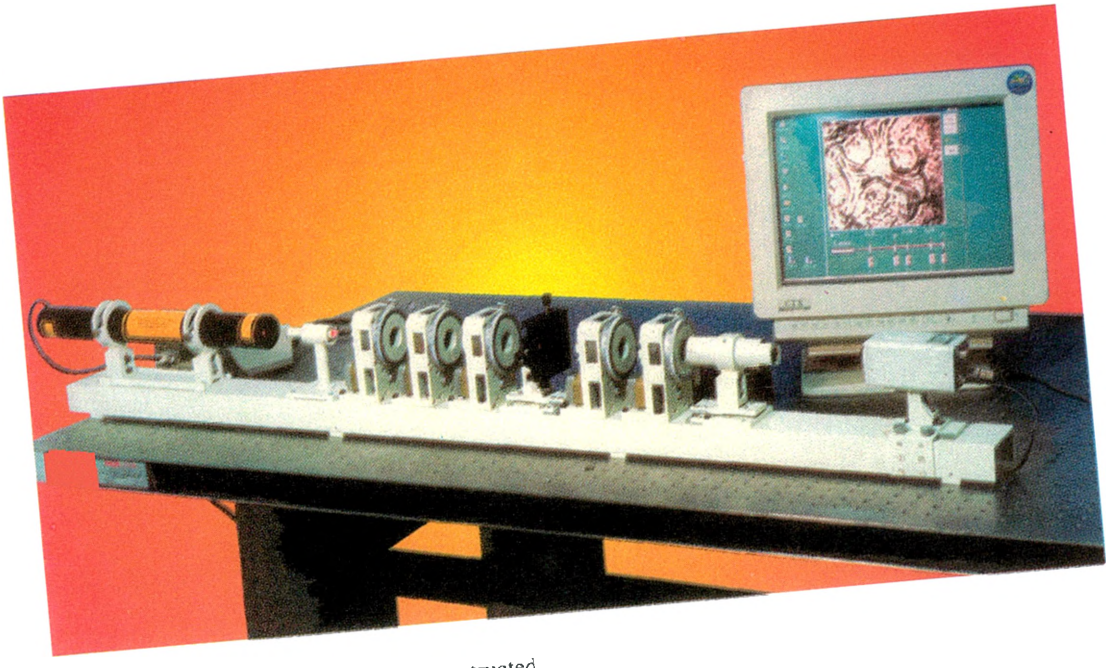

Fig. 2. Photograph of the polarimeter constructed.

– the half-wave plate is rotated to obtain the maximum signal level registered by the CCD matrix (without saturation),

– both the analyser and the second quarter-wave plate are rotated into the crossed position with the polariser.

The measuring procedure, after inserting a sample and selecting its image area, comprises the following tasks:

– Isoclinic lines studies. With polariser and analyser crossed (quarter-wave plates are coupled with polariser and analyser, the tissue sample is illuminated by linearly polarised light), polariser and analyser are rotated together with quarter-wave plates within the range of 90°. The system records 60 images of isoclinic lines. The angular increment between the adjacent images is equal to 1.5°.

– Isochromatic lines studies: optical axes of quarter-wave plates are rotated by 45° with respect to polariser and analyser transmission planes (circular polarisation of the light incident on the sample under test). One image is registered.

– For a selected birefringent element, the phase change introduced by this element is measured in the field of view by rotating one of the quarter-wave plates. The rotation angle corresponding to the minimum detector signal in the image area permits the change of phase to be determined.

The registration of the set of images of isoclinic lines and the image of isochromatic lines, as well as the quarter-wave rotation for phase determination, are conducted automatically. The option of simultaneous automatic measurement of isoclinic and isochromatic lines is feasible as well.

The signal from the keyboard starts the correlation programs developed by the group of the Chair of Correlation Optics from Ukraine.

2. Correlation analyses of changes in the phase-azimuth structure of biological tissue

2.1. Theoretical model

The muscular tissue is a structured system of protein bundles representing, from the optical point of view, a two-component amorphously (actin) crystalline (miosin) matrix [1]–[4]. Optical properties of such a system can be completely described by the superposition of matrix operators of the corresponding components:

$$\{M\} = \{A\} + \{K\} = \begin{Vmatrix} a_{11}+k_{11} & a_{12} & 0 & 0 \\ a_{21} & a_{22}+k_{22} & k_{23} & k_{24} \\ 0 & k_{32} & a_{33}+k_{33} & k_{34} \\ 0 & k_{42} & k_{43} & a_{44}+k_{44} \end{Vmatrix} \tag{1}$$

where a_{ik}, k_{mn} are elements of the corresponding Mueller matrices [5], [6].

While passing through such a structure, the polarized laser beam with the azimuth α_0 forms an object field with the following parameters:

$$\alpha = 0.5 \arctan\left[\frac{\cos 2\alpha_0 k_{32} + \sin 2\alpha_0 (a_{33} + k_{33})}{a_{21} + \cos 2\alpha_0 (a_{22} + k_{22}) + \sin 2\alpha_0 k_{23}}\right],$$

$$\beta = 0.5 \arcsin(\cos 2\alpha_0 + \sin 2\alpha_0 k_{43}). \tag{2}$$

The coordinate distribution of such a field intensity, which can be seen through the analyzer, oriented at the angle Ω with respect to the incidence plane, is written as follows:

$$I(X, Y) = I_0[\cos^2(\alpha - \Omega) + \sin^2(\alpha - \Omega)\tan^2\beta]. \tag{3}$$

On the other hand, such a field represents a superposition of the components

$$I(X, Y) = \Psi(X, Y) + T(X, Y) \tag{4}$$

where $\Psi(X,Y)$, $T(X,Y)$ – are the field components formed by myosin and actin components of the muscular tissue, correspondingly.

It can be seen from the analysis of relations (1)–(4) that the vector structure of such components is sufficiently different. Additionally, the partial field of the actin component is linearly polarized. It is possible to show that orienting the polarizer at the angle

$$\Omega^* = \frac{\pi}{2} + 0.5 \arctan\left(\frac{\sin 2\alpha_0 a_{33}}{a_{21} + \cos 2\alpha_0 a_{22}}\right), \tag{5}$$

the component $T(X,Y)$ can be compensated practically to a zero-level by forming the system of polarizophotes (the lines of zero-intensity) in the coherent image of muscular tissue. In this process, the intensity distribution of a myosin component will change to the following level:

$$\Psi^*(X, Y) = 0.5\,\Psi(X, Y)\left\{\cos^2\left[\frac{\sin 2\alpha_0 k_{33} + \cos 2\alpha_0 k_{32}}{\sin 2\alpha_0 k_{32} + \cos 2\alpha_0 k_{22}}\right]\right.$$

$$\left. + \sin^2\left[\frac{\sin 2\alpha_0 k_{33} + \cos 2\alpha_0 k_{32}}{\sin 2\alpha_0 k_{32} + \cos 2\alpha_0 k_{22}}\right] \times \tan[0.5 \arcsin(\cos 2\alpha_0 + \sin 2\alpha_0 k_{43})]\right\}. \tag{6}$$

The interrelation between myosin and actin protein components and their biochemical exchange play the main part in the movability and the contraction of muscular tissue; these factors are sufficient in the life of a human being. Pathological changes in the physiology of such biotissues lead to a decrease or disappearance of relative density of actin proteins which cause the dystrophy of muscles or their necrosis (the infarct of the tissue).

Early optical diagnostics of such processes includes:

– obtaining a coherent image of a muscular tissue,

– polarization selection of myosin and actin polarization images together with their visualization,

– correlation processing of the above images,

– wavelet analysis of their structure.

2.2. Correlation processing of polarization images

The idea of the method is based on statistic processing of intensity distributions $\psi(X,Y)$, $T(X,Y)$ in different experiment polarization situations by defining the coefficient of the autocorrelation of the corresponding images [7]

$$r = \frac{\sigma_{\Psi,\tilde{\Psi}}}{\sigma_{\Psi}\sigma_{\tilde{\Psi}}}, \tag{7}$$

where $\sigma_{\Psi,\tilde{\Psi}}$ is the covariance of two masses of intensities in coherent biotissue images, being compared by means of autocorrelation; σ_{Ψ}, $\sigma_{\tilde{\Psi}}$ are the dispersions of the intensities of the corresponding parts of polarization images being analyzed. We have

$$\sigma_{\Psi,\tilde{\Psi}} = \frac{1}{m \cdot n} \sum_{i=0}^{m-1} \sum_{j=0}^{n-1} (\Psi_{i,j} - \overline{\Psi}) \cdot (\tilde{\Psi}_{i,j} - \overline{\tilde{\Psi}}), \tag{8}$$

$$\sigma_{\Psi}^2 = \frac{1}{m \cdot n} \sum_{i=0}^{m-1} \sum_{j=0}^{n-1} (\Psi_{i,j} - \overline{\Psi})^2, \tag{9}$$

$$\sigma_{\tilde{\Psi}}^2 = \frac{1}{m \cdot n} \sum_{i=0}^{m-1} \sum_{j=0}^{n-1} (\tilde{\Psi}_{i,j} - \overline{\tilde{\Psi}})^2, \tag{10}$$

$$\overline{\Psi} = \frac{1}{m \cdot n} \sum_{i=0}^{m-1} \sum_{j=0}^{n-1} (\Psi_{i,j}), \tag{11}$$

$$\overline{\tilde{\Psi}} = \frac{1}{m \cdot n} \sum_{i=0}^{m-1} \sum_{j=0}^{n-1} (\tilde{\Psi}_{i,j}). \tag{12}$$

The calculated totality of the correlation coefficients for every selection of intensities masses for the horizontal and vertical directions gives the autocorrelation function $G(\psi\psi)$ of the laser polarization image of the biotissue.

2.3. Experimental investigations and discussion

Figure 3 presents the coherent images of physiologically normal muscular tissue of rat's heart (left column) and the necrotically (infarct) changed one (right column), obtained for parallel (Fig. 3**a**, **b**) and crossed (Fig. 3**c**, **d**) polarizer-analyzer directions.

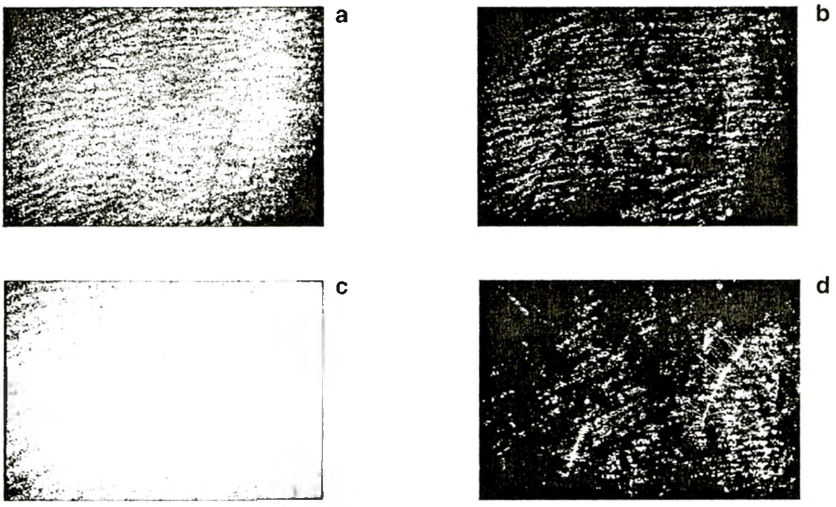

Fig. 3. Coherent images of muscle tissues.

It can be seen that morphological structures of the tissues of both types represent the system of ordered and oriented muscular bundles. The highest contrast structure can be observed in the configuration with the polarizer and analyzer being crossed, consistent with a given model of optically oriented uniaxial fibers.

Figure 4 illustrates a series of dependences of ACFs (autocorrelation functions) $G(\psi, \psi)$ of coherent images of such tissues.

The obtained ACFs has the following common properties:

– All ACFs possess the extremum corresponding to a white noise (at the origin of the coordinate system).

– While increasing the shift coordinates (m, n) of the coherent image the functions $G(\psi\psi)$ decrease quickly. This proves its decorrelation related to the peculiarities of the morphological structure of the muscular tissue.

The comparative analysis of the ACF series of images of the tissues of A and B groups has shown high-frequency quasi harmonic component. It modulates the functions $G(\psi\psi)$ of a physiologically normal muscular heart tissue (Fig. 4**d**). The modulation parameters correspond to a characteristic morphological size (~2 μm) in the coherent image. For necrotically changed tissue there is no such a component in ACF of its polarization image. The peculiarity observed can be connected with the polarization visualization of the structure of the actin component in the fibers of the muscular tissue (Eq. (6)).

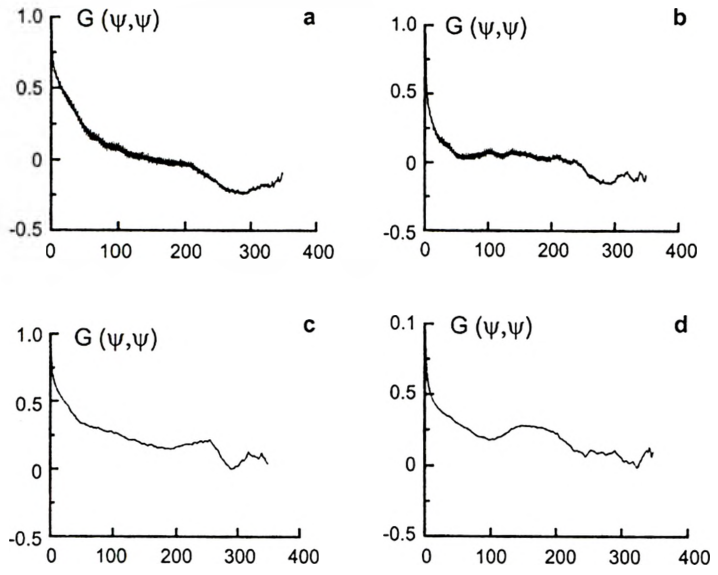

Fig. 4. ACFs of the images of muscle tissues.

In physiologically normal fibers the coordinate distribution of such a protein is equidistant and looks like crosscut discs of the diameter of 1–3 μm [4]. That is why in the crossed polarizer-analyzer configuration such an image component appears to be a system of equidistant zero-intensity stripes (polarizophotes), which are perpendicular to the direction of the myosin bundle. Correspondingly, the additional modulated component connected with the actin component is formed in the coherent image in the background of the myosin component autocorrelation structure.

On the contrary, the degenerative-dystrophic changes in the muscular tissue structure cause degeneration of the actin. This is manifested in an increase of the intensity of the corresponding polarizophote images. That is why the modulation amplitude of the ACF decreases or disappears in the case of infarct of the muscular tissue (Fig. 4**a**, **c**). Such processes can be analyzed in more detail by calculating the power spectrum $J(\psi, \psi)$ [7] of the series of ACF of polarization images of the biotissues being diagnosed.

Figure 5 presents the spectra $J(\psi, \psi)$ of the coherent images of physiologically normal muscular tissue of rat's heart (Fig. 5**a**, **b**) and necrotically (infarct) changed (Fig. 5**c**, **d**) one, obtained with the parallel (Fig. 5**a**, **c**) and crossed (Fig. 5**b**, **d**) polarizer and analyzer directions.

It can be seen from the data given that there is a distinct difference among them in the high-frequency part of the spectrum for the crossed polarizer–analyzer configuration. The localized spectral extremum (Fig. 5**a**, **b**) corresponds to the quasi -harmonic actin component of the coherent image of physiologically normal tissue. The spectrum $J(\psi, \psi)$ is smooth for the necrotically changed muscular tissue; it proves practically complete degradation of the actin. On the other hand, the degenerative

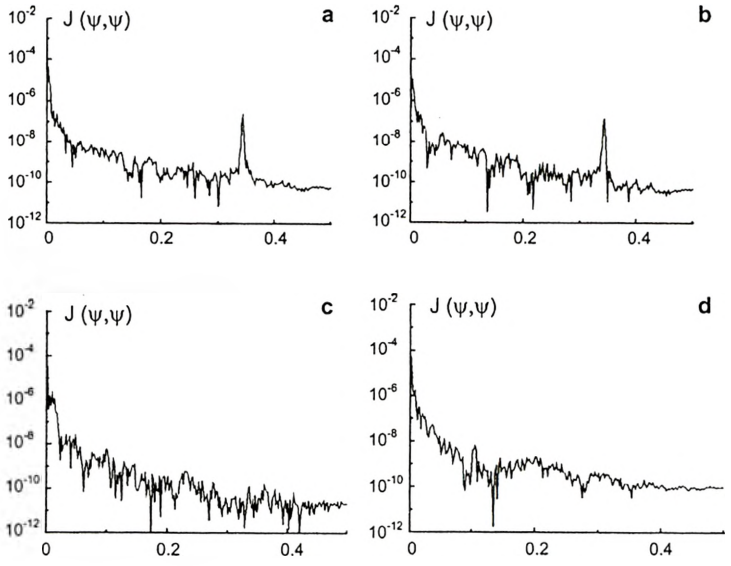

Fig. 5. Densities of power spectra.

-dystrophic changes of the biotissue morphological structure are spatially localized in many cases. The effectiveness of the correlation processing, inherent to the instrument, is inadequate for such pathologies, because of the large amount of averaging of random intensity values.

Figure 6 shows the results of the wavelet-analysis of coherent images of physiologically normal muscular tissue of the rat's heart obtained with parallel (Fig. 6**a**) and crossed (Fig. 6**b**) polarizer–analyzer directions. Figure 7 illustrates identical results for the necrotically changed (infarct) tissue.

From the data obtained it can be seen that:

– In the case of parallel polarizer and analyzer directions, the distribution of extreme values of coefficients c_{jk} of the intensity distribution $\psi(X)$ of the wavelet transform of coherent images of physiologically normal and pathologically changed biotissues is concentrated in the small-scale part. It is rather smooth and weakly -fluctuating over the remaining part.

– In the crossed polarizer–analyzer configuration the extrema of the wavelet -transform coefficients are observed practically for all scales of the function $\xi_{jk}(X)$ over the whole coordinate space. In the part corresponding to the polarization image analysis using a low-frequency window a local extremum of the coefficients c_{jk} is observed. The latter is practically equal to zero for small scales.

The results obtained can be connected with the peculiarities of the morphological structure of muscular tissues. For the samples of both types one can observe a fibrous layering rather than a homogeneous area. Such a peculiarity leads to rather smooth

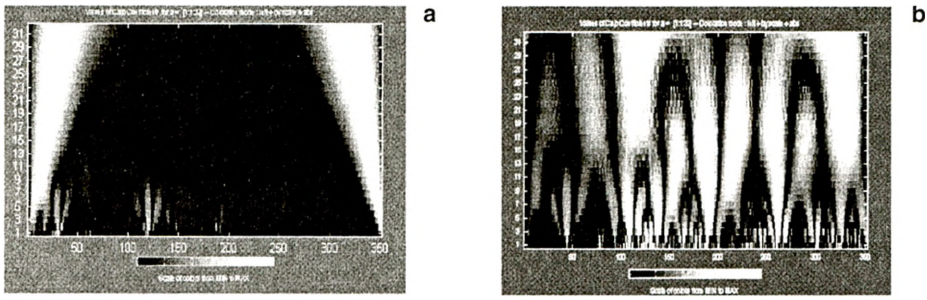

Fig. 6. Wavelet analysis of coherent images of physiologically normal muscle tissue sample.

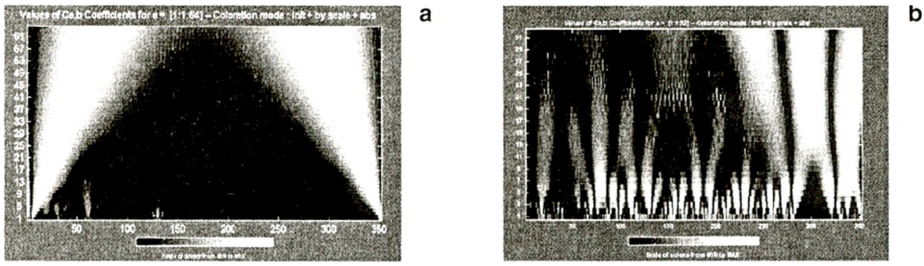

Fig. 7. Wavelet analysis of coherent images of pathologically changed muscle tissue sample.

distribution of space frequencies in the corresponding coherent images. But the high level of the light-scattered background in the images obtained with parallel polarizer and analyzer directions "hides" low-frequency component of the object. As a result, the wavelet analysis shows only the distribution of high-frequency intensity structure of the corresponding images. Polarization filtering of such images gives maximum contrast in the images of oriented muscular bundle systems. Correspondingly, the peculiarities of their space structure in the plane of the histological section can be more distinctly observed due to a decrease of high-level scattered light background. This leads to an increase of fluctuations of the wavelet-transform coefficients of intensity dependences in such images.

There is a part of infarct affection – a destruction of the fibers for necrotically changed muscular tissue. From the point of view of optics, it is a low-frequency image with practically zero intensity due to the loss of anisotropic properties of the protein substance. The wavelet-transform has the extremum for large-scale coefficients of the polarization filtered image. On the contrary, there is no high-frequency structure of the coherent image of necrotically changed part; it is shown by the zero-values of the small-scale coefficients c_{jk}.

The complex polarization-correlation and wavelet analysis of the changes in the microstructure of muscular tissues illustrates the possibilities of the laser polarimetry technique in early diagnostics of pathology appearance and determining its location.

References

[1] TUCHIN V.V., Proc. SPIE **1884** (1993), 234.
[2] TUCHIN V.V., Usp. Fiz. Nauk **167** (1997), 517 (in Russian).
[3] VICHLJAEVA E.M., *Clinical Gynaecology* (in Russian), Medicina 1997.
[4] RAJCH G., *Collagen* (in Russian), Medicina 1969.
[5] ASTAFEVA N.M., Usp. Fiz. Nauk **166** (1996), 1147.
[6] USHENKO A.G., BURKOVETS D.M., YERMOLENKO S.B., ARKHELYUK A.D., PISHAK V.P., YUZKO A.M., PISHAK O.V., PLAVIUK L.A., PERESUNKO A.P., ZNACK V.M., Proc. SPIE **3904** (1999), 527.
[7] USHENKO A.G., BURKOVETS D.M., YERMOLENKO S.B., ARKHELYUK A.D., USHENKO YU.A., PISHAK V.P., PISHAK O.V., GRIGORISHIN P.M., ZIMNAYKOV D.A., Proc. SPIE **3904** (1999), 542.

Received June 3, 2002